

# CrystEngComm

Accepted Manuscript



This is an *Accepted Manuscript*, which has been through the Royal Society of Chemistry peer review process and has been accepted for publication.

*Accepted Manuscripts* are published online shortly after acceptance, before technical editing, formatting and proof reading. Using this free service, authors can make their results available to the community, in citable form, before we publish the edited article. We will replace this *Accepted Manuscript* with the edited and formatted *Advance Article* as soon as it is available.

You can find more information about *Accepted Manuscripts* in the [Information for Authors](#).

Please note that technical editing may introduce minor changes to the text and/or graphics, which may alter content. The journal's standard [Terms & Conditions](#) and the [Ethical guidelines](#) still apply. In no event shall the Royal Society of Chemistry be held responsible for any errors or omissions in this *Accepted Manuscript* or any consequences arising from the use of any information it contains.

Cite this: DOI: 10.1039/c0xx00000x

www.rsc.org/xxxxxx

ARTICLE TYPE

# Critical factors influencing the structures and properties of metal-organic frameworks

Kang Shen, Mingdao Zhang, Hegen Zheng\*

*Received (in XXX, XXX) XthXXXXXXXXXX 20XX, Accepted Xth XXXXXXXXXXXX 20XX*

DOI: 10.1039/b000000x

Metal-organic frameworks (MOFs) have emerged as an important family of compounds that have fascinating structures and diverse applications. But until now, targeted synthesis of MOFs with desired frameworks is still a challenge. In order to appreciate the properties and to design new frameworks, it is necessary to understand how to rationalize the design and synthesis of MOFs from a fundamental perspective. This highlight review will outline the recent advances on this topic from both our and other groups and provide an overview of different factors influencing on the structures of MOFs. These examples illustrate some of present trends concerning the design of the organic ligands and SBUs, coordination assemblies, experimental conditions.

## 1. Introduction

In the last two decades, the design and construction of novel MOFs (metal-organic frameworks) which use a minimum amount of material to build maximum surface areas with fine control over pore size has attracted great interest, not only for their fascinating variety of architectures and topologies,<sup>1-3</sup> but also for their potential applications in molecular adsorption and separation processes,<sup>4-5</sup> ion exchange,<sup>6</sup> catalysis,<sup>7-8</sup> sensor technology,<sup>9</sup> optoelectronics and so on.

Because of its wide breadth of application to advanced materials, controlled synthetic methods, ligands with various coordination modes, and the influences of various factors upon structures have come to prominence in this field.<sup>10-13</sup> For the chemist, MOFs syntheses could be considered as “block-building games”: the final architecture depends on the building modules and their compatibilities. Analyses of the final geometries, of the diverse interactions and optimization of the growth processes are described as “crystal engineering”.<sup>14</sup> MOFs are constructed mainly by coordination bonds between metal ions and ligands, together with other intermolecular interactions. The arrangement of the components in coordination polymers mostly only exist in the solid state: metal ions and organic ligands interact through coordination interactions and weaker forces in solution giving some small building blocks, and then, by self-assembly processes, MOFs grow based on the same interactions.<sup>15-16</sup> Metal ions and organic ligands are generally called nodes and linkers. The variety of “nodes and linkers” offers infinite possibilities for building new species with wonderful architectures and topologies. Much work has been devoted to the synthesis, structural characterization, and properties of MOFs. In this process, the accumulation of sufficient experimental data allows chemists to proceed beyond the random studies and to derive some useful laws of assembly. Towards this end, several effective synthetic strategies such as “node-and-spacer” and “secondary

building units (SBUs)” have been successfully established and developed. But the control of product structure still remains a challenge in this field due to the fact the self-assembly process is effected by various external physical or chemical factors including counterion,<sup>17</sup> template, temperature,<sup>18</sup> pressure, solvent,<sup>19</sup> and pH value, etc. In this contribution, we will introduce the factors including the positional isomerism, substituents and spacers of organic ligands, SBUs, solvents, metal ions and so on that make prominent influence on the formation, structure and property of MOFs.

## 2. Assembly strategies of organic ligands in the construction of MOFs

According to different coordinating groups, organic ligands can be divided into several categories, such as carboxylate ligands, N-containing heterocyclic ligands (pyridyl ligands, pyrrol ligands, imidazolyl ligands and so on), cyano ligands, phosphoryl ligands, sulfonyl ligands and so on. Among these various organic ligands, carboxylate ligands are often selected as multifunctional organic linkers because of their abundant coordination modes to metal ions, allowing for various structural topologies and because of their ability to act as H-bond acceptors and donors to assemble supramolecular structures.<sup>20</sup> Compared with carboxylate ligands, the coordination pattern of N-containing heterocyclic ligands is unitary and the controllability of the structure of the target compound is higher. For attaining novel structures, mixed ligands are also a good choice for the construction of new polymeric structures. Use of a second bridging ligand to extend the metal carboxylate systems is one of the common ways to obtain higher dimensional networks. To date, a large number of mixed-ligand MOFs have been reported<sup>21-22</sup> revealing that the combination of different ligands can result in greater tenability of structural frameworks than single ligands. The ligands containing imidazole or pyridine are regarded as important auxiliary ligands in the

design and assembly of metal–organic coordination polymers.

## 2.1 Positional isomeric effect

Ligands with the same coordination groups but locating at different positions may lead to significant positional isomerism to affect the structural assemblies of MOFs.

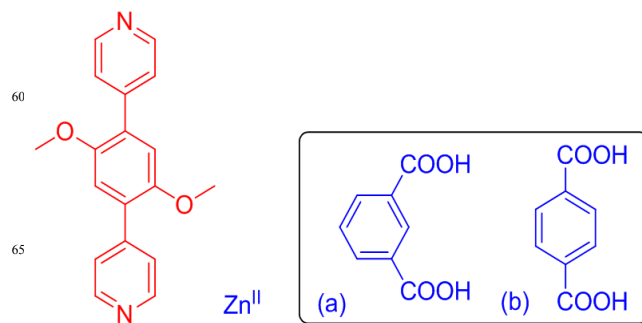
For example, two aromatic dicarboxylic acids H<sub>2</sub>IPA (isophthalic acid) (Scheme 1a) and H<sub>2</sub>TPA (terephthalic acid) (Scheme 1b), possessing an angle-increased binding tendency, are active in regulating the structural assemblies of MOFs.<sup>23</sup> Rigid linear ligands L (4,4'-(2,5-dimethoxy-1,4-phenylene)dipyridine) incorporating with two carboxyl-containing auxiliary ligands H<sub>2</sub>IPA and H<sub>2</sub>TPA have been adopted to build two complexes with Zn<sup>II</sup> under solvothermal conditions. In {[Zn(L)(IPA)]<sub>n</sub> (**1**), the H<sub>2</sub>IPA ligands link the Zn<sup>II</sup> ions to form a 1D chain. Such 1D chains are further extended through L ligands from nearly perpendicular direction to furnish a 2D layer (Fig. 1a). When H<sub>2</sub>IPA is replaced with H<sub>2</sub>TPA, the resulting {[Zn(L)(TPA)]·DMF}<sub>n</sub> (**2**) shows a 3D supramolecular structure (Fig. 1b).

To further systematically investigate the influence of the positional isomeric ligands on the structures and properties of transition metal complexes, F. P. Huang and H. D. Bian *et al.*<sup>24</sup> reported a series of Cd<sup>II</sup> coordination polymers based on the mixed-ligand system of dipyridyl ligand: 3,3'-bpt (1*H*-3,5-bis(3-pyridyl)-1,2,4-triazole) (Scheme 2) and three positional isomeric phenyl dicarboxylate anions: *o*-BDC (1,2-benzenedicarboxylate anion), *m*-BDC (1,3-benzenedicarboxylate anion) and *p*-BDC (1,4-benzenedicarboxylate anion) (Scheme 2, a-c), namely, [Cd<sub>4</sub>(*p*-BDC)<sub>4</sub>(3,3'-bpt)<sub>4</sub>]·9H<sub>2</sub>O (**3**), [Cd(*m*-BDC)(3,3'-bpt)(H<sub>2</sub>O)]·2H<sub>2</sub>O (**4**), [Cd(*o*-BDC)(3,3'-bpt)(H<sub>2</sub>O)]·(3,3'-bpt)·4H<sub>2</sub>O (**5**). Complex **3** possess a two dimensional (2D) layer structures (Fig. 2a). Complex **4** presents an infinite one dimensional (1D) tubular-like chain (Fig. 2b). Complex **5** displays a 2D honeycomb structure consisting of a 1D metal–organic helical chain (Fig. 2c). Structural diversities indicate that the nature of isomeric benzene–dicarboxylates ligands plays crucial roles in modulating structures of these complexes.

## 2.2 Substituent effect

The substituents of organic ligands probably influence the network structures of MOFs in two aspects.<sup>25</sup> On the one hand, they may possess additional interconnecting functions to extend the coordination motifs, in view of their ability to form coordination and secondary interactions such as H-bonding and aromatic stacking. On the other hand, those inert substituents may impose remarkable steric and/or electronic effects on the binding properties of organic ligands, and consequently, the network structures of the resulting MOFs.

A series of Co<sup>II</sup>, Zn<sup>II</sup> MOFs have been constructed by selecting TPOM (tetrakis(4-pyridyl)methane) incorporated with deprotonated 1,3-H<sub>2</sub>bdc (isophthalic acid), 5-OH-H<sub>2</sub>bdc (5-hydroxyisophthalic), 1,3,5-H<sub>3</sub>btc (benzene-1,3,5-tricarboxylic) and 1,2,4,5-H<sub>4</sub>btc (benzene-1,2,4,5-tetracarboxylic) (Scheme 3, a-d)<sup>26</sup> as building blocks respectively. For instance, in {[Co<sub>2</sub>(TPOM)(bdc)<sub>2</sub>(H<sub>2</sub>O)<sub>2</sub>]·(H<sub>2</sub>O)<sub>3</sub>]<sub>n</sub> (**6**), each Co atom coordinates to TPOM to form infinitely a wave-like 2D network along the *b* axis. There are two types of coordination environments around the Co<sup>II</sup> ions. The bdc<sup>2-</sup> anions link two Co



**Scheme 1** Illustration of assembled system with Zn<sup>II</sup>, L, H<sub>2</sub>IPA (a), H<sub>2</sub>TPA (b).

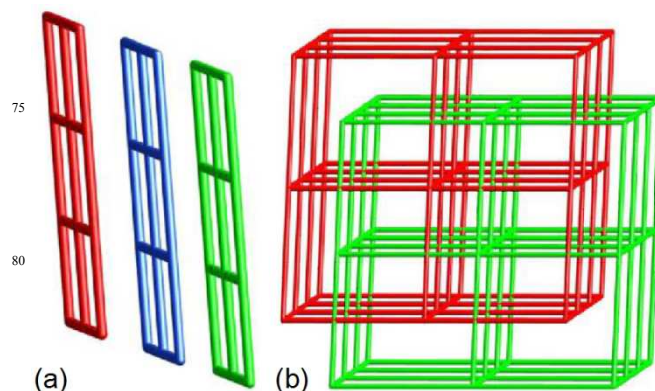
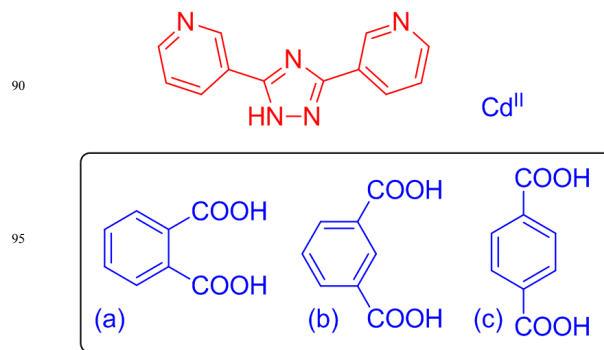


**Fig. 1** (a) View of single 2D coordination networks in **1**. (b) Schematic representation of 2-fold interpenetrating 3D framework with pcu topology of **2**.



**Scheme 2** Illustration of the mixed-ligand assembled system with Cd<sup>II</sup>, 3,3'-bpt, and three isomeric aromatic dicarboxylic acids, including: (a) *o*-BDC, (b) *m*-BDC, (c) *p*-BDC.

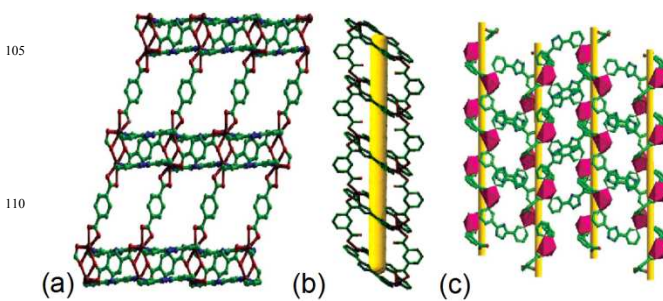
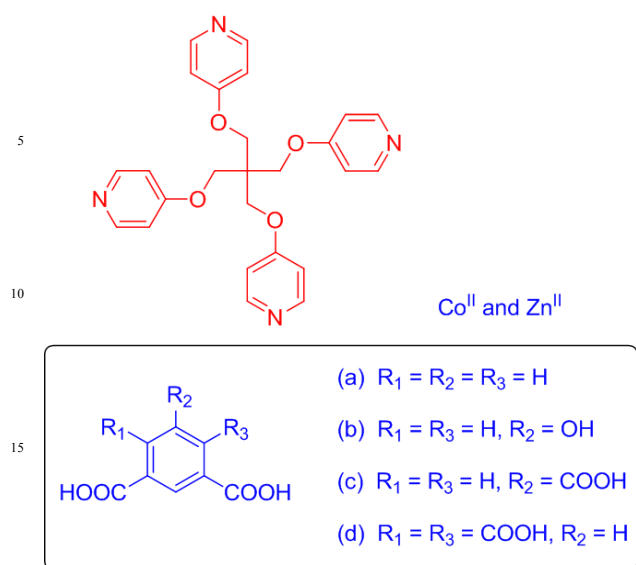


**Fig. 2** Three Cd<sup>II</sup> MOFs combining mixed ligands (a) 3,3'-bpt/*p*-BDC (**3**), (b) 3,3'-bpt/*m*-BDC (**4**) and (c) 3,3'-bpt/*o*-BDC (**5**).



**Scheme 3** Illustration of the mixed-ligand assembled system with Co<sup>II</sup>/Zn<sup>II</sup>, TPOM, and a series of comparable R-isophthalic acids with different substituents, including: (a) 1,3-H<sub>2</sub>bdc, (b) 5-OH-H<sub>2</sub>bdc, (c) 1,3,5-H<sub>3</sub>btc, (d) 1,2,4,5-H<sub>4</sub>btc.

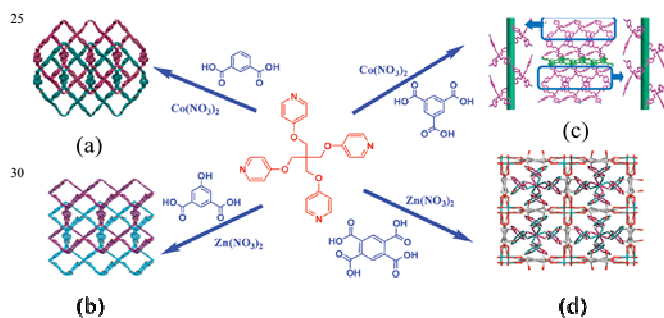
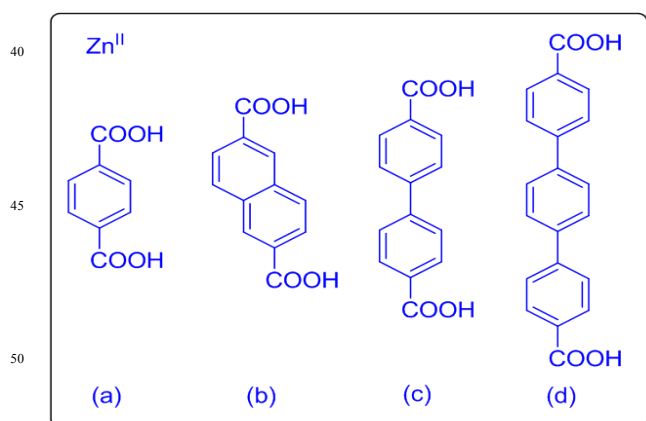


**Fig. 3** Various Co<sup>II</sup> and Zn<sup>II</sup> coordination networks of **6** (a), **7** (b), **8** (c), **9** (d) assembled from TPOM and a series of benzene-dicarboxylic acids.



**Scheme 4** Illustration of the assembled system with Zn<sup>II</sup> and a series of aromatic dicarboxylic acids including: (a) H<sub>2</sub>BDC, (b) 2,6-H<sub>2</sub>NDC, (c) H<sub>2</sub>BPDC, (d) H<sub>2</sub>TPDC.

atoms belonging to different 2D networks to form a 3D framework. The potential voids are large enough to be filled via

mutual interpenetration of an independent equivalent framework, generating a 2-fold interpenetrating 3D architecture (Fig. 3a). Complex  $\{[Zn_2(TPOM)(5-OH-bdc)_2] \cdot (DMF)(H_2O)_2\}_n$  (**7**) possess similar 2-fold interpenetrating three-dimensional (3D) framework with **bbf** topology, but complex **6** crystallizes in an achiral space group (*P2/c*), and complex **7** crystallizes in chiral space group (*P2*). In comparison with complex **6**, although the phenolic hydroxyl group do not engaged in metal coordination, it will significantly change the electronic density of the ligand as an electron-donating group (Fig. 3b). Complex  $\{[Co_3(TPOM)(btc)_2(H_2O)] \cdot (H_2O)_4\}_n$  (**8**) reveals a 3D framework with binuclear Co clusters, which displays weak antiferromagnetic character. The carboxylate groups of btc<sup>3-</sup> adopt three different coordination modes: one is chelating in a bidentate mode, another is bridging bidentate, and the third is monodentate bridging mode (Fig. 3c). In compound  $\{[Zn_2(TPOM)(btc)_2]\}_n$  (**9**), the completely deprotonated btc<sup>4-</sup> anions link four Zn atoms through the carboxylate coordination to form a 3D framework with larger open channels and it is the first example of TPOM as a counteraction (Fig. 3d).

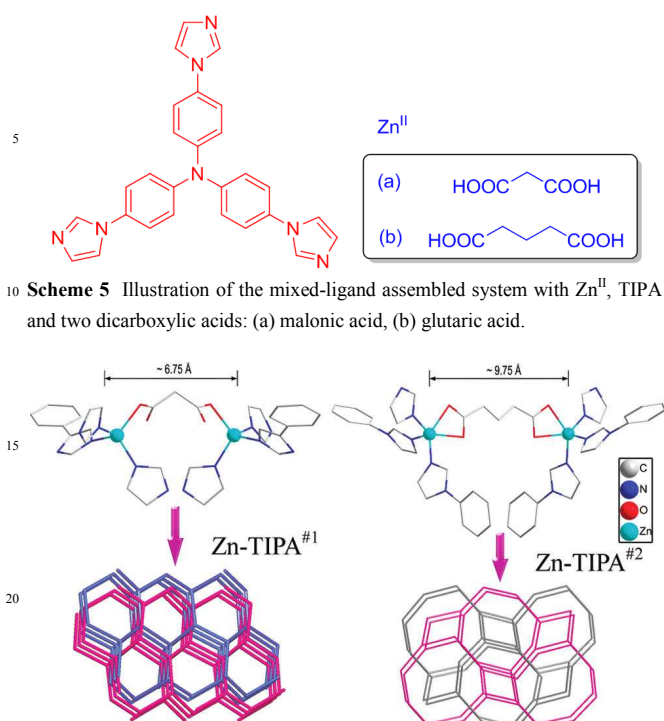
### 2.3 Spacer effect

In principle, rigid linkers tend to construct 3D open networks with available cavities. With the increase of spacer length, interpenetration of such nets generally occurs to decrease the empty volumes of the crystal lattices. In contrast, flexible spacers may promote the generation of distorted frameworks, leading to dynamic micro porous MOFs that can shrink or expand upon external stimuli.<sup>27</sup>

A family of conjugated aromatics spacers can be used to design the longer rigid ligands. For example, O. M. Yaghi *et al.*<sup>28</sup> found that diffusion of triethylamine into a solution of zinc nitrate and H<sub>2</sub>BDC (Scheme 4a) in *N,N'*-dimethylformamide/chlorobenzene resulted in landmark complex  $Zn_4O(BDC)_3 \cdot (DMF)_8 \cdot (C_6H_5Cl)$  (**10**) which has been named MOF-5.<sup>29</sup> After that, they obtained a series of H<sub>2</sub>BDC derivatives: 2,6-H<sub>2</sub>NDC, H<sub>2</sub>BPDC and H<sub>2</sub>TPDC (Scheme 4b-d) by introducing the spacers between the carboxyl groups of BDC. They assembled these aromatic dicarboxylic ligands with Zn<sup>II</sup> to get an IRMOF series based on the prototype of MOF-5 which has been constructed from octahedral Zn-O SBU and BDC<sup>2-</sup>.

Regarding the changes of spacers with aliphatic groups, flexible carboxylic ligands such as malonic acid and glutaric acid can be obtained. Based on Zn<sup>2+</sup> and mixed-ligands of a N-centered extended tripod ligand (tris(4-(1*H*-imidazol-1-yl)phenyl)amine, TIPA) and two flexible aliphatic carboxylic acids (malonic acid and glutaric acid) (Scheme 5a-b), two novel zinc coordination polymers<sup>30</sup> containing two unusual Zn-TIPA substructures (Zn-TIPA<sup>#1</sup> in **11** and Zn-TIPA<sup>#2</sup> in **12**) with (10,3)-d and (10,3)-a topology have been successfully synthesized. Both complexes **11** and **12** feature (3,4)-connected non-interpenetrated 3D frameworks (Fig. 5). If the malonic and glutaric ligands are neglected from the structures, two 2-fold interpenetrated (10,3) topological networks can be observed, the incorporation of malonic and glutaric ligands further reinforce the stability of **11** and **12**.

Recently, Z. Q. Shi and H. G. Zheng *et al.*<sup>31</sup> reported a series of MOFs, namely,  $\{[Zn(BPBP)_{0.5}(hfipbb)]\}_n$  (**13**),  $\{[Zn(BPBP)(trans-chdc)] \cdot H_2O\}_n$  (**14**),  $\{[Zn_2(BPBP)(4,4'-sdb)_2]\}_n$



**Scheme 5** Illustration of the mixed-ligand assembled system with  $\text{Zn}^{\text{II}}$ , TIPA and two dicarboxylic acids: (a) malonic acid, (b) glutaric acid.

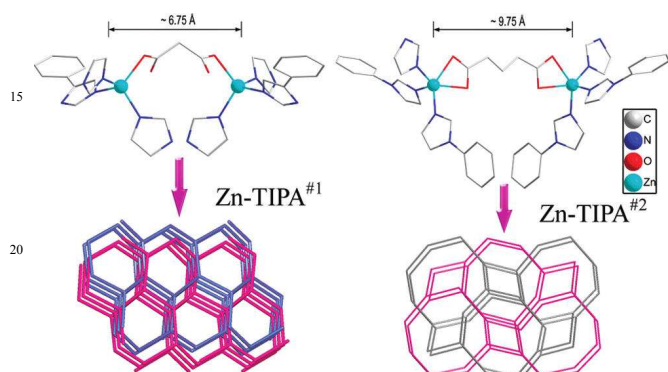


**Fig. 5** The scheme demonstrates the evolution from (10,3)-d  $\text{Zn-TIPA}^{\#1}$  subnet (left) in **11** to (10,3)-a  $\text{Zn-TIPA}^{\#2}$  subnet (right) in **12**, achieved by increasing the length of flexible aliphatic dicarboxylic acid.

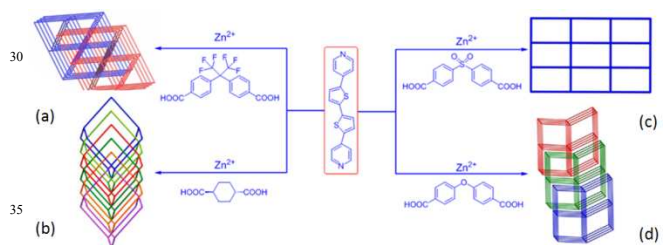
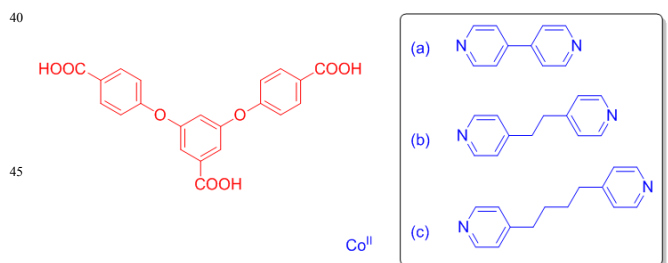


**Fig. 6** Various  $\text{Zn}^{\text{II}}$  coordination networks of **13** (a), **14** (b), **15** (c), **16** (d) that assembled from BPBP and a series of dicarboxylic acids.



**Scheme 6** Illustration of the mixed-ligand assembled system with  $\text{Co}^{\text{II}}$ ,  $\text{H}_3\text{BCPBA}$  and bipyridine ligands including: (a) bipy, (b) bpe, (c) bpp.

(**15**), and  $\{[\text{Zn}_2(\text{BPBP})(\text{oba})_2] \cdot \text{H}_2\text{O} \cdot \text{DMA}\}_n$  (**16**) on the basis of a bipyridine ligand BPBP and different multicarboxylate-type coligands. (BPBP = 5,5'-bis(4-pyridyl)-2,2'-bithiophene,  $\text{H}_2\text{hfipbb}$  = 4,4'-(hexafluoroisopropylidene)bis(benzoic acid),  $\text{trans-H}_2\text{chdc}$  = *trans*-1,4-cyclohexanedicarboxylic acid, 4,4'- $\text{H}_2\text{sdb}$  = 4,4'-sulfonyldicarboxylic acid,  $\text{H}_2\text{oba}$  = 4,4'-oxybis(benzoic acid)) (Fig. 6). Complex **13** is a 3D supramolecular architecture with 3-

fold interpenetration (Fig. 6a). Two crystallographically equivalent  $\text{Zn}^{\text{II}}$  cations are bridged by four carboxylate groups adopting a bis-bidentate coordination mode to generate a dinuclear  $\text{Zn}^{\text{II}}$  “paddle-wheel” type secondary building unit (SBU). This  $[\text{Zn}_2(\text{CO}_2)_4]$  unit is interesting and rarely observed in other coordination compounds, the paddle-wheel is bridged by  $\text{hfipbb}$  ligands to form a 2D undulating (4, 4) network with rhomb-like windows and the SBU  $[\text{Zn}_2(\text{CO}_2)_4]$  can be regarded as a 6-connected node. The whole framework of complex **13** can be topologically represented as a rare 6-connected **mab** net with the vertex symbol of  $\{4^4 \cdot 6^{10} \cdot 8\}$ . In complex **14**, the carboxylate groups of the *trans*-chdc ligands link the  $\text{Zn}^{\text{II}}$  cation centers into an infinite 1D zigzag chain, such 1D zigzag chains are further linked by the BPBP ligands, leading to the formation of a 3D framework. The 3D structure of complex **14** can be clarified as a classical 4-connected diamond (**dia**) lattice by considering  $\text{Zn}^{\text{II}}$  cations as the 4-connected nodes and all ligands as the 2-connected spacers. Notably, the large channel in a single framework has an approximate pore size of  $18.82 \text{ \AA} \times 26.16 \text{ \AA}$ , which allows the other five identical 3D single frameworks to penetrate and, thus, affords a 6-fold interpenetrating architecture (Fig. 6b). In complex **15**, the completely deprotonated 4,4'-sdb ligand shows a bidentate coordination mode. Pairs of  $\text{Zn}^{\text{II}}$  cations are joined by two symmetrical 4,4'-sdb ligands to generate a dinuclear  $\text{Zn}^{\text{II}}$  “paddle-wheel” type secondary building unit (SBU). These paddle-wheel SBUs are further bridged through the second terminal carboxylate group of the symmetrical 4,4'-sdb ligands into a 1D chain. Then the BPBP ligands join all infinite 1D chains into a 2D layer (Fig. 6c). The 2D network can be simplified to a **sql** net. In complex **16**, the  $\text{Zn}^{\text{II}}$  cations are linked through the oba ligands to form 2D layers, such resulting layers are further connected by BPBP ligands, leading to the formation of a 3D framework (Fig. 6d). Complex **16** represents a  $\{4^{12} \cdot 6^3\}$   $\alpha$ -Po **pcu** topology by using BPBP and oba ligands as linkers.

Various base-type bridging ligands, involving paired pyridine, imidazole and triazole groups with different spacers in between, have also been applied to react with angular rigid carboxylic acids to form well-defined MOFs, which can be regulated by the spacer effect of ligands. For example, a series of flexible bipyridine ligands such as bipy, bpe, bpp (Scheme 6a-c) assemblies with  $\text{H}_3\text{BCPBA}$  and  $\text{Co}^{\text{II}}$  afford three different MOFs  $\{[\text{Co}(\text{HBCPBA})(\text{bipy}_{0.5})_2(\text{H}_2\text{O})]\}_n$  (**17**),  $\{[\text{Co}_3(\text{BCPBA})_2(\text{bpe})(\mu_2\text{-H}_2\text{O})_4] \cdot 2\text{DMF}\}_n$  (**18**),  $\{[\text{Co}_2(\text{HBCPBA})_2(\text{bpp})(\mu_2\text{-H}_2\text{O})_2] \cdot \text{H}_2\text{O} \cdot 2\text{DMF}\}_n$  (**19**).<sup>32</sup> In complex **17**, the  $\text{Co}^{\text{II}}$  ions can be regarded as 4-connected nodes with all crystallographically independent bipy ligands acting as 2-connected linkers, and the  $\text{HBCPBA}^{2-}$  ligands acting as V-shaped linkers. Therefore, the whole structure can thus be reduced as a (4, 4) sheet (Fig. 7a). To evaluate the role of ligand in the self-assembly of organic–inorganic hybrid frameworks, the reaction with bpe is carried out to afford complex **18**. The structure of **18** is a pillared 2-fold interpenetrating 3D  $\rightarrow$  3D network. Two pillared 3D motifs, identical in structure interpenetrate to yield a new type of catenated network consisting of large, open, one-dimensional (1D) channels (Fig. 7b). When bpe was replaced by bpp, a structurally different complex **19** is obtained. In complex **19**, the two  $\text{Co}^{\text{II}}$  atoms are bridged by a water molecule to form a binuclear cluster. Each binuclear  $\text{Co}^{\text{II}}$  is connected by three

HBCPBA<sup>2-</sup> anions and two bpp to form a 2D net structure (Fig. 7c).

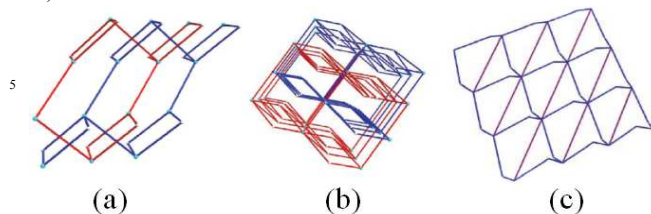


Fig. 7 (a) Schematic representation of the 2D → 2D framework by two identical sheets in **17**. (b) Schematic representation of the 3D → 3D framework by two identical sheets in **18**. (c) View of the 2D net structure of **19**.

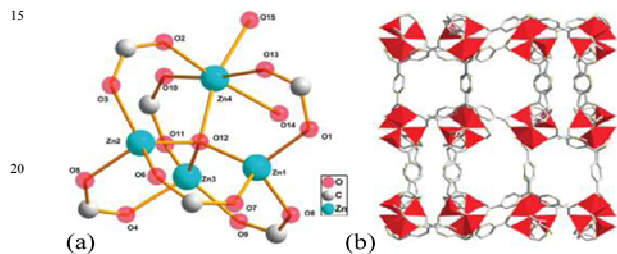


Fig. 8 (a) View of the  $[Zn_6(\mu_6-O)]$  cluster in **20**. (b) 1D micropore along the *a* axis in **20**.

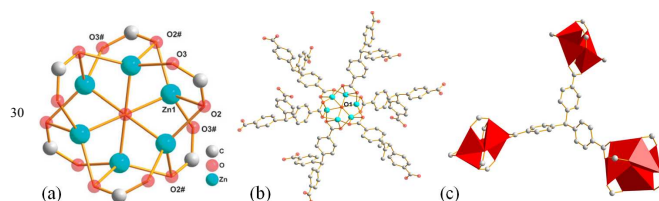


Fig. 9 (a) A view of the  $[Zn_6(\mu_6-O)(CO_2)_6]$  cluster in **21**. (b) - (c) are coordination environment of the  $Zn^{II}$  ion in **21**.

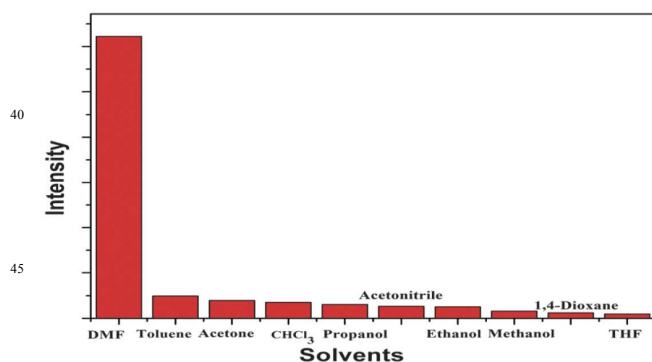


Fig. 10 The PL intensities of **21** introduced to various pure solvents when 50 excited at 390 nm.

### 3. Structures of MOFs based on different secondary building units

Most of metal-organic frameworks are produced by organic 55 ligands as linkers to coordinate to metals or metal cluster as nodes or molecular building blocks. In order to get large pore materials, the usual way to do this is extending the organic

ligands, but in practice they are often found to be highly interpenetrated and have low porosity. To solve the problem, 60 Yaghi and co-workers developed an efficient strategy for the construction of frameworks with the use of SBUs replace single metal ions in the MOFs, giving the structures with high stability and without a tendency to interpenetrate.<sup>33</sup>

Choosing appropriate SBUs have an important significance for 65 the construction of MOFs: First of all, predicting the topology of the target products through the configuration of SBUs as well as the coordination modes of organic ligands; Secondly, the use of multiple metal ions in a cluster bridged by multiple coordinating ligands tends to enhance the robustness of the MOFs; Thirdly, 70 making MOFs to possess optical and electrical properties by introduction of metal centers with superior physical properties. SBUs as the node of the construction of MOFs directly affect MOFs' structures by their coordination geometry. According to the composition of SBUs, the types of SBUs could be divided 75 into metal-oxygen-based cluster and W-Cu-S-based cluster. SBUs are essential to the design of directionality for the construction of MOFs and to the achievement of robust frameworks.

#### 3.1 Metal-oxygen-based cluster polymers

80 Metal-oxygen-based SBUs have been widely researched and reported such as tetranuclear  $[Zn_4O(COO)_6]$ <sup>34,5</sup> and dinuclear  $[Cu_2(COO)_4]$ <sup>35</sup>, these SBUs are used as 6-connected octahedral nodes and 4-connected tetragonal nodes respectively in self-assembly reactions. Many robust MOFs have been synthesized 85 based on transition metals carboxylate SBUs which usually comprise two, three, four or more metal centers.

J. H. Cui and H. G. Zheng *et al.*<sup>36</sup> reported a 3D non-interpenetrated 90 framework  $\{[Zn_4O(TCOPM)_2(H_2O)_2] \cdot 8H_2O \cdot 3DMF\}_n$  (**20**) (TCOPM = tris-*p*-carboxyphenyl)-methane) which was obtained from self-assembly of  $H_3TCOPM$  and Zn nitrate. The TCOPM anions all adopt a bidentate coordination mode to bridge two Zn centers. Zn1, Zn2, and Zn3 reside in tetrahedral environments, and each coordinates by three carboxylate oxygen atoms from different 95 TCOPM ligands and one  $\mu_4-O$  atom at the center of the cluster. The Zn4 ion adopts an octahedral coordination geometry surrounded by the  $\mu_4-O$  atom, three carboxylate oxygen atoms, and another two oxygen atoms from two water molecules. The four Zn ions form a distorted tetrahedron around  $\mu_4-O$  (Fig. 8a). The TCOPM ligand acts as a 3-connected node. A  $\mu_4-oxo$  bridged 100  $Zn_4O$  cluster is bridged by six carboxylate groups from six TCOPM<sup>3-</sup> units to provide the octahedron-shaped secondary building unit (SBU), which extends infinitely to give 6-connected nets (Fig. 8b).

They also reported a MOF,<sup>37</sup> namely,  $[Zn_{12}(\mu_6-O)_2(TCOPM)_4] \cdot 3H_2O \cdot 8NO_3 \cdot 8DMF$  (**21**) based on  $[Zn_6(\mu_6-O)(CO_2)_6]$  cluster with pores for the first time. The core of the cluster consists of a single O ( $\mu_6-O$ ) atom bonded to six Zn atoms, forming a regular  $[Zn_6(\mu_6-O)]$  polyhedron. The two oxygen atoms 110 of each carboxylate from TCOPM<sup>3-</sup> are all coordinated with three Zn atoms (Fig. 9a).  $[Zn_6(\mu_6-O)(CO_2)_6]$  cluster acts as six-connected SBU (Fig. 9b) and TCOPM<sup>3-</sup> acts as a triangular organic building block (Fig. 9c). For complex **21**, it could be used as a chemical sensor for sensing of small molecules. The intensity 115 of the PL in complex **21** depends on the identity of the guest

molecule, with DMF > toluene > acetone > CHCl<sub>3</sub> > propanol > acetonitrile > ethanol > methanol > 1,4-dioxane > THF (Fig. 10), which is probably due to the majority of chromophores in complex **21** being exposed to the different solvents, and they have different interactions with solvents from each other. Another similar zinc MOF [Zn<sub>6</sub>(μ<sub>6</sub>-O)(TPO)<sub>2</sub>](NO<sub>3</sub>)<sub>4</sub>·3H<sub>2</sub>O (**22**) (H<sub>3</sub>TPO = tris(4-carboxylphenyl)phosphineoxide) based on the same SBUs ([Zn<sub>6</sub>(μ<sub>6</sub>-O)(CO<sub>2</sub>)<sub>6</sub>] (Fig. 9a) is reported.<sup>33</sup> The coordination mode of organic ligand H<sub>3</sub>TPO is similar to the ligand H<sub>3</sub>TCOPM which acts as a triangular building block in MOF, so they have the same topology type: the **pyr** form of FeS<sub>2</sub>.

In addition to the above MOFs with symmetrical six Zn centers SBU, J. H. Cui and H. G. Zheng *et al.*<sup>38</sup> reported another non-interpenetrating porous Zn-MOF namely [Zn<sub>5</sub>(μ<sub>3</sub>-OH)<sub>4</sub>L<sub>2</sub>]·7H<sub>2</sub>O·DMF (**23**) (H<sub>3</sub>L = 3,5-bis(4-carboxyphenoxy)benzoic acid) with the decorated **tfz-d** topology based on Zn<sub>6</sub>O<sub>2</sub> and H<sub>3</sub>L as ligand (Fig. 11). The Zn<sub>6</sub>O<sub>2</sub> clusters consist of two Zn<sub>3</sub>O, and the cores of the clusters consist of a single O (μ<sub>3</sub>-OH) atom bonded to three Zn atoms, forming a regular Zn<sub>3</sub>O tetrahedron structure. Zn1 is bound to two carboxylate O atoms from two L<sup>3-</sup> ligands and four μ<sub>3</sub>-hydroxy groups, and Zn2 is bound to four carboxylate O atoms from four L ligands and two μ<sub>3</sub>-hydroxy groups. Both Zn1 and Zn2 give octahedral structures, while Zn3 are bridged by two carboxylate O atoms from two L<sup>3-</sup> ligands and two μ<sub>3</sub>-hydroxy groups to give tetrahedral structures (Fig. 12).

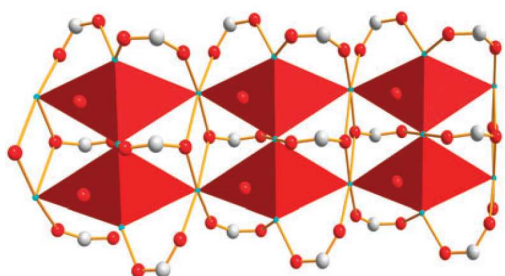


Fig. 11 View of the tetrahedron-shaped SBU in **23**.

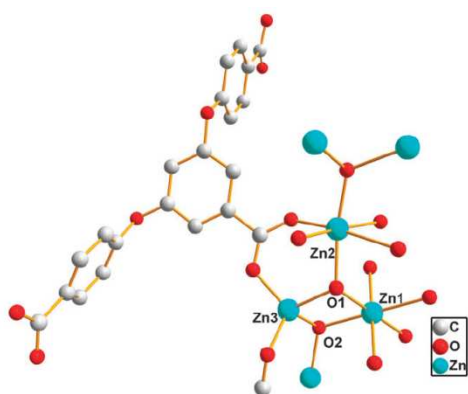


Fig. 12 Coordination environment of the Zn<sup>II</sup> ion in **23**.

### 3.2 W-Cu-S-based cluster polymers

In contrast to the metal-oxygen SBUs, the W-S-Cu SBUs have more variable central cores. For example, one [WS<sub>4-n</sub>O<sub>n</sub>]<sup>2-</sup> (n = 0-2) core chelates a certain number of Cu<sup>+</sup> ions to form the basic SBUs, the number and arrangement of the Cu<sup>+</sup> ions around the

[WS<sub>4-n</sub>O<sub>n</sub>]<sup>2-</sup> (n = 0-2) core can be varied by changing the synthesis conditions, and different combinations of [WS<sub>4-n</sub>O<sub>n</sub>]<sup>2-</sup>

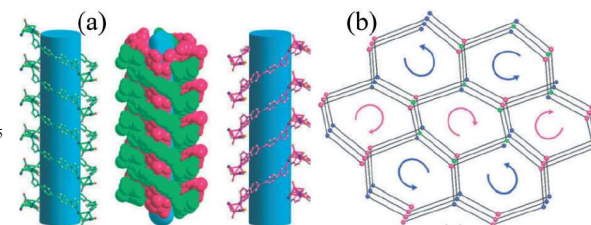


Fig. 13 (a) Schematic representation of the channels consisting of a left-handed helix and a right-handed helix in **24**. (b) Schematic representation of a single (10,3)-bths net along the a axis in **24**, the left/right-handed helices are illustrated as pink and blue arrows, respectively.

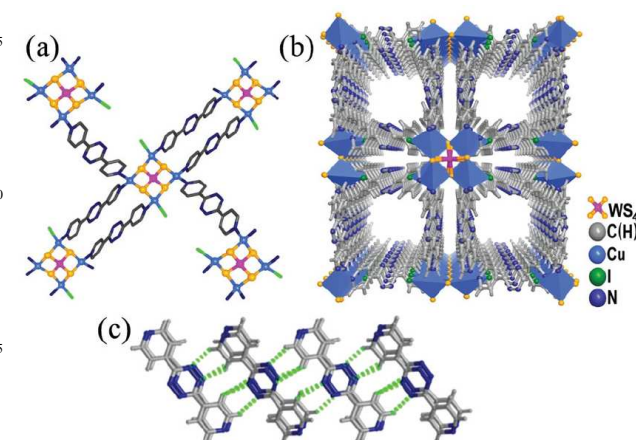


Fig. 14 (a) Coordination environment of the [WS<sub>4</sub>Cu<sub>4</sub>]<sup>2-</sup> unit in **25**. (b) Perspective view of the nanotubular structure of **25**. (c) Hydrogen bonds between paired ligands of the interpenetrating networks (green dashed lines).

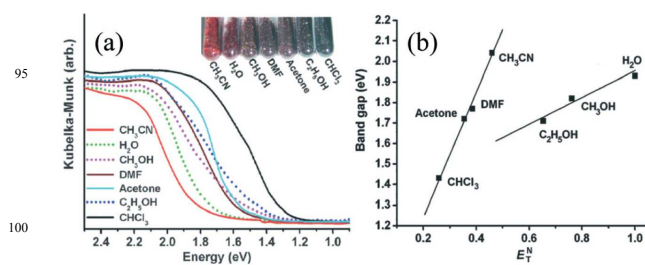


Fig. 15 (a) UV-vis spectra and photograph of the inclusion complex **25** with different solvents. (b) Band gaps of the inclusion complexes versus solvent  $E_T^N$  values.

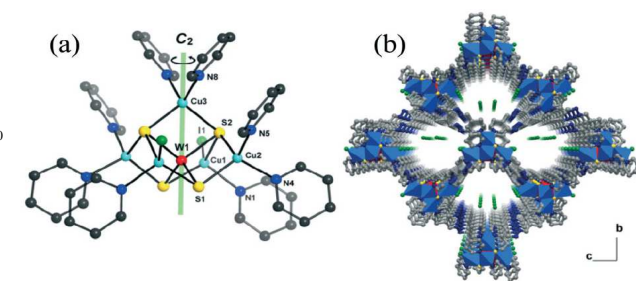
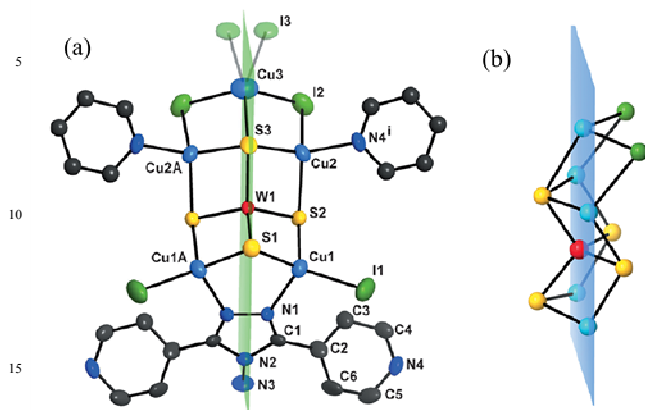
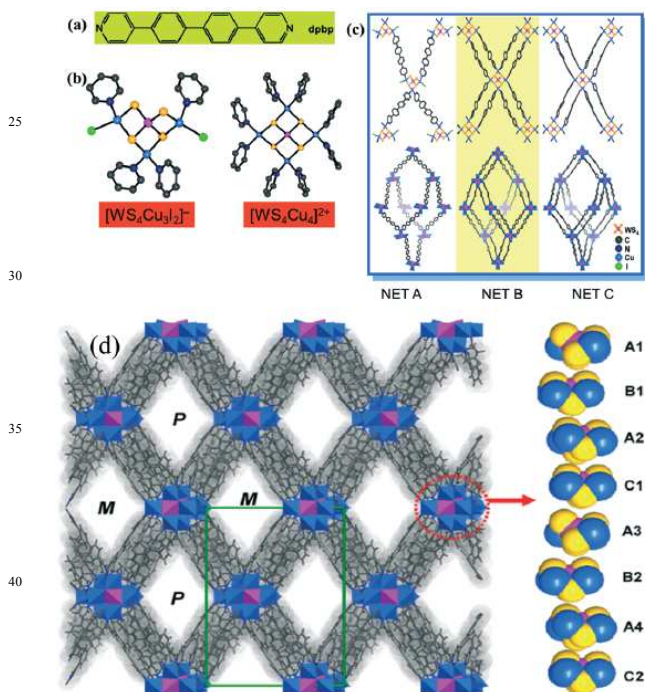


Fig. 16 (a) Coordination environment of the [WS<sub>4</sub>Cu<sub>5</sub>]<sup>3+</sup> unit in **26**. (b)

Nanotubular structure of **26** (H atoms and the solvent guests are omitted for clarity).



**Fig. 17** (a) Coordination environment of the [WS<sub>4</sub>Cu<sub>5</sub>]<sup>3+</sup> unit in **27**. (b) Side view of the [WS<sub>4</sub>Cu<sub>5</sub>]<sup>3+</sup> unit shows the coplanarity of the five Cu<sup>+</sup> ions and the W atom.



**Fig. 18** (a) Structure of the dpbp ligand. (b) Coordination environments in the [WS<sub>4</sub>Cu<sub>3</sub>I<sub>2</sub>]<sup>-</sup> and [WS<sub>4</sub>Cu<sub>4</sub>]<sup>2+</sup> SBUs in **28**. (c) Basic units in NET A (left), NET B (middle) and NET C (right). (d) Left: nanotubular structure of **28**. Right: space filling model showing the close packing of the SBUs of the eight frameworks.

(n = 0–2) and Cu<sup>+</sup> afford SBUs with different geometries and connectives.<sup>39</sup> The nuclear numbers of cluster SBUs from 3 to 7 have been reported,<sup>40–48</sup> so the W–S–Cu SBUs could be able to coordinate to more ligands compared with metal–oxygen SBUs.

In 2011, X. Q. Yao and H. G. Zheng *et al.*<sup>49</sup> reported a (10,3)-type W–Cu–S cluster polymer, named {[WOS<sub>3</sub>Cu<sub>3</sub>Br(TIPA)](H<sub>2</sub>O)(DMF)}<sub>n</sub> (**24**), based on the TIPA (tris(4-(1H-imidazol-1-yl)phenyl)amine) organic linker and the [WOS<sub>3</sub>Cu<sub>3</sub>]<sup>+</sup> SBU (Fig. 13). The (10,3)-type MOFs usually have

large channels, of which some also feature chirality (i.e. the net with (10,3)-a, srs topology).<sup>50</sup>

A nanotubular metal–organic framework (MOF), {[WS<sub>4</sub>Cu<sub>4</sub>]<sub>2</sub>(dptz)<sub>3</sub>DMF}<sub>n</sub> (**25**) [dptz = 3,6-di-(pyridin-4-yl)-1,2,4,5-tetrazine] with a pentanuclear [WS<sub>4</sub>Cu<sub>4</sub>]<sup>2+</sup> unit (Fig. 14a) has been reported by Z. Z. Lu and H. G. Zheng *et al.*<sup>45</sup> The [WS<sub>4</sub>Cu<sub>4</sub>]<sup>2+</sup> units, acting as tetrahedral nodes, are linked by two paired ligands and two single ligands with four adjacent units into a diamondoid network. Six diamondoid networks associate together with the [WS<sub>4</sub>Cu<sub>4</sub>]<sup>2+</sup> units of each net arranged parallel, forming square-shaped nanotubes along the c direction (Fig. 14b). Strong C–H⋯N hydrogen bonds are formed between the paired dptz ligands of the interpenetrated networks with an average C⋯N distance of 3.291(2) Å, which stabilizes the overall nanotubular architecture (Fig. 14c). The complex **25** shows solvatochromic behavior when immersed in solvents ranging in polarity from water to chloroform (Fig. 15a). The band gaps of these solvent-included complexes are in linear correlation with the polarity of the guest solvents (Fig. 15b). The solvent molecules can be sensed by the changes in the UV-vis spectra of the corresponding inclusion compounds, showing a new way of signal transduction as a new kind of sensor.

Z. Z. Lu and H. G. Zheng *et al.*<sup>41</sup> reported a 3D metal–organic framework, [(WS<sub>4</sub>Cu<sub>5</sub>)I<sub>2</sub>(dpmh)<sub>4</sub>]<sub>n</sub><sup>+</sup>·n<sup>-</sup>·n-solvent (**26**) (dpmh = (1E,2E)-1,2-bis(pyridin-4-ylmethylene)hydrazine). This polymer contains one-dimensional channels (Fig. 16b) formed in four-fold interpenetrating diamondoid networks with a hexanuclear [WS<sub>4</sub>Cu<sub>5</sub>]<sup>3+</sup> unit as the SBU (Fig. 16a), which has a square-pyramidal geometry and acts as a tetrahedral node. In the same paper, another polymer [(WS<sub>4</sub>Cu<sub>5</sub>)I<sub>5</sub>(Hdpta)<sub>4</sub>]<sub>n</sub><sup>-</sup>·n(C<sub>2</sub>H<sub>5</sub>)<sub>4</sub>N<sup>+</sup>·nDMF·n-solvent (**27**) (Hdpta = 2,5-di(pyridin-4-yl)-1H-pyrrol-1-amine) was also documented. This polymer contains a brick wall-like layer with a hexanuclear [WS<sub>4</sub>Cu<sub>5</sub>]<sup>3+</sup> unit as the SBU (Fig. 17a). This [WS<sub>4</sub>Cu<sub>5</sub>]<sup>3+</sup> unit is a new type of [WS<sub>4</sub>Cu<sub>x</sub>]<sup>x-2</sup> cluster unit in which the five Cu<sup>+</sup> ions are in one plane with the W atom, forming a planar unit (Fig. 17b).

The above-mentioned MOFs are the same type that only one kind of SBU in MOF, also some MOFs with the coexistence of two kinds of SBUs. For example, Z. Z. Lu and H. G. Zheng *et al.*<sup>50</sup> reported a 3D framework, {[WS<sub>4</sub>Cu<sub>4</sub>(dpbp)<sub>4</sub>]<sup>2+</sup>·[WS<sub>4</sub>Cu<sub>3</sub>(dpbp)<sub>2</sub>I<sub>2</sub>]<sup>-</sup>]<sub>n</sub>·x-solvent (**28**), based on a long rod-like ligand dpbp (4,4'-di(4-pyridyl)-biphenyl), which is more than twice the length of 4,4'-bipyridine (Fig. 18a). In complex **28**, the anionic net is formed by the tetranuclear [WS<sub>4</sub>Cu<sub>3</sub>I<sub>2</sub>]<sup>-</sup> SBU, and the cationic net is formed by the pentanuclear [WS<sub>4</sub>Cu<sub>4</sub>]<sup>2+</sup> SBU, forming an unprecedented 8-fold non-equivalent interpenetrated structure (Fig. 18b). The anionic framework [WS<sub>4</sub>Cu<sub>3</sub>(dpbp)<sub>2</sub>I<sub>2</sub>]<sup>-</sup>, named NET A, is constructed by the tetranuclear [WS<sub>4</sub>Cu<sub>3</sub>I<sub>2</sub>]<sup>-</sup> unit (Fig. 18c). The four cationic frameworks contain two independent groups of [WS<sub>4</sub>Cu<sub>4</sub>(dpbp)<sub>4</sub>]<sup>2+</sup>, named as NET B and NET C, which are built by a pentanuclear [WS<sub>4</sub>Cu<sub>4</sub>]<sup>2+</sup> SBU (Fig. 18c). Large rhombus-shaped tubes with diagonal dimensions of ~20 × 10 Å are formed in spite of the high interpenetration (Fig. 18d).

## 4. Other factor influencing the assembly of MOFs

### 4.1 Solvent

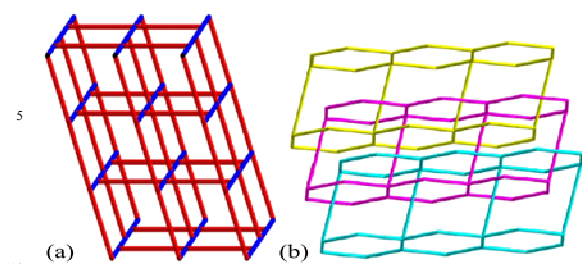


**Fig. 19** (a)  $6^5 8$  topology of  $\text{CdSO}_4$ -type structure of **29**. (b) 3-fold 2D  $\rightarrow$  2D parallel interlock structure of **30**.

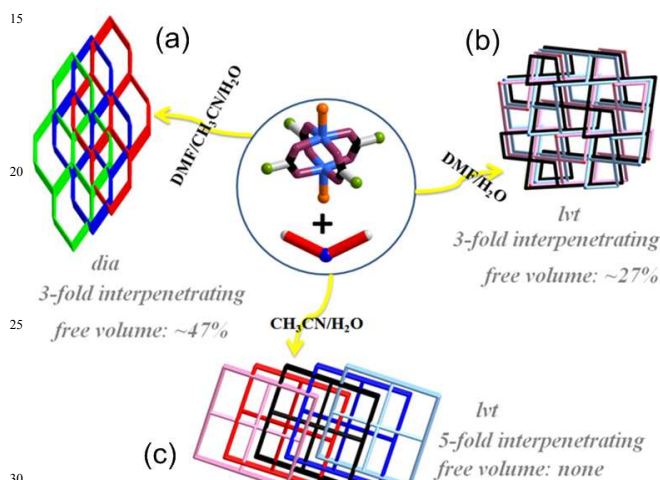


**Fig. 20** The topologies of **31** (a), **32** (b), **33** (c).

Two unusual solvent-controlled MOFs<sup>51</sup> have been obtained from the solvothermal assemblies of  $\text{H}_2\text{L}$  (4,4'-dicarboxydiphenylamine) and BIP (4,4'-bis(imidazol-1-yl)phenyl) with  $\text{Co}^{\text{II}}$  nitrate in DMF- $\text{H}_2\text{O}$  and  $\text{CH}_3\text{CN}$ - $\text{H}_2\text{O}$  solvents, respectively. A 3D non-interpenetrated framework  $[\text{Co}_2(\text{L})_2(\text{BIP})_2 \cdot 3\text{H}_2\text{O}]_n$  (**29**) can be prepared in DMF- $\text{H}_2\text{O}$ . Two  $\text{L}^{2-}$  connect two  $\text{Co}^{\text{II}}$  atoms to achieve a 28-membered  $[\text{Co}_2(\text{L})_2]$  metallocyclic ring. These rings are further connected through their corners forming 1D wave-like ladder-chain structures. BIP double lines linking the parallel  $[\text{Co}_2(\text{L})_2]$  chains in two different directions give rise to a 3D framework net. Closer examination of the structure of complex **29** reveals that the framework adopts the  $\text{CdSO}_4$  (**cds**) topology, a 4-connected  $6^5 8$  net, as shown in Fig. 19a. When using  $\text{CH}_3\text{CN}/\text{H}_2\text{O}$  instead of DMF/ $\text{H}_2\text{O}$  as solvent,  $[\text{Co}(\text{L})(\text{BIP})(\text{H}_2\text{O}) \cdot 2\text{CH}_3\text{CN}]_n$  (**30**) possessing unusual 3-fold 2D  $\rightarrow$  2D poly catenation of (4,4) nets is obtained (Fig. 19b). The BIP ligand links neighboring  $\text{Co}^{\text{II}}$  ions to form an infinitely 1D zigzag chain. The  $\text{L}^{2-}$  anions link these zigzag chains to form ladder-like 2D sheets. The 2D sheet contains a larger channel so that the large dimensions and corrugated nature of the net allow them to interpenetrate in an extensive and unusual fashion.

By a systematic variation of solvent, three unprecedented novel MOFs<sup>52</sup> are obtained:  $[\text{Cu}_2(\text{L})_2(\text{H}_2\text{O})_2 \cdot 3/2\text{H}_2\text{O}]_n$  (**31**) (DMF- $\text{CH}_3\text{CN}$ - $\text{H}_2\text{O}$ ) with three-fold interpenetrated **dia** topology (Fig. 20a);  $[\text{Cu}(\text{L})(\text{DMF}) \cdot 5/2\text{H}_2\text{O}]_n$  (**32**) (DMF- $\text{H}_2\text{O}$ ) with three-fold interpenetrated **lvt** topology (Fig. 20b), and  $[\text{Cu}(\text{L})(\text{H}_2\text{O}) \cdot \text{H}_2\text{O}]_n$

(**33**) ( $\text{CH}_3\text{CN}$ - $\text{H}_2\text{O}$ ) with five-fold interpenetrated **lvt** topology

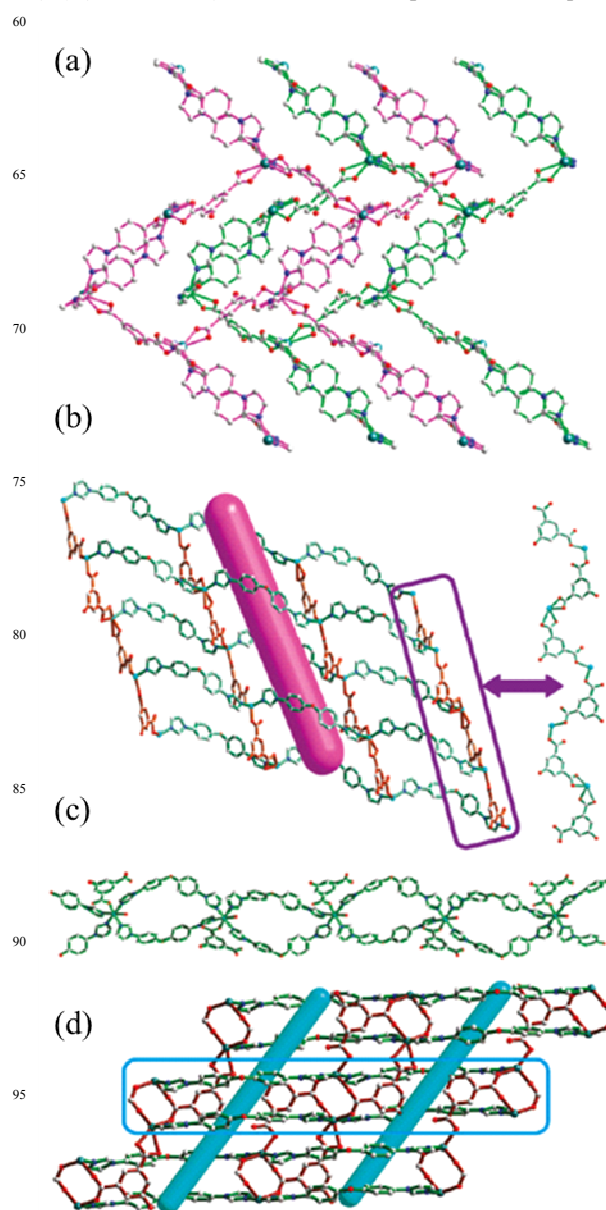


**Fig. 21** (a) Views of the 2D sheets by BIDPE ligands, 5-OH- $\text{bdc}^{2-}$ ,  $\text{Cd}^{\text{II}}$  or  $\text{Co}^{\text{II}}$ . (b) Views of the wavelike 2D framework by 5-OH- $\text{bdc}^{2-}$ , BIDPE and  $\text{Zn}^{\text{II}}$ . (c) Views of the 1D double-stranded chain by 5-OH- $\text{bdc}^{2-}$ , BIDPE and  $\text{Ni}^{\text{II}}$ . (d) Views of the 2D framework by 5-OH- $\text{bdc}^{2-}$ , BIDPE and  $\text{Mn}^{\text{II}}$ .

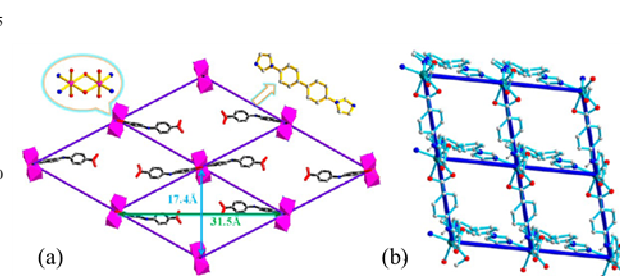


**Fig. 22** (a) Schematic representation of the (4, 4) network in **34**. (b) Views of the (4, 4) sheets of **35** and **36**.

(Fig. 20c) ( $H_2L = 4,4'$ -dicarboxydiphenylamine). The  $H_2L$  ligands assemble with metal clusters to form the four-connected paddle-wheel SBUs. Comparing the synthesis system of the above MOFs, there are no other synthesis conditions change but the solvents, so the polarity of the solvent ( $CH_3CN < DMF < H_2O$ ) is significantly important to determine the constructing structures.  $H_2L$  is a flexible V-shaped ligand, the  $L^{2-}$  anions can perform with different configurations, regulating the solvent can effectively generate the desirable architectures and topologies, and also adjust the porosity of frameworks.

#### 4.2 metal ion

As one of the most common factors influencing the assembly of MOFs, metal ions can be viewed as a family of controllable building blocks. One particular metal element with a given valence normally defines its intrinsic coordination preference and geometry.

A series of mixed-ligand MOFs have been prepared under diffusion condition, by assembling  $Cd^{II}$ ,  $Co^{II}$ ,  $Zn^{II}$ ,  $Ni^{II}$ ,  $Mn^{II}$  nitrate with BIDPE and 5-OH- $H_2bdc$ .<sup>53</sup> These MOFs display various 2D and 3D structural patterns with different coordination geometries of the metal ions, clearly indicating the metal-directed assembly. In  $Cd^{II}$ ,  $Co^{II}$ ,  $Zn^{II}$  MOFs, though the metal centers take different coordination numbers (4 and 6) and geometries (octahedron, trigonal bipyramid and tetrahedron), they are bridged by 5-OH- $H_2bdc$  to afford 2D sheets (Fig. 21a-b). For the  $Ni^{II}$  MOFs, the neighboring  $Ni^{II}$  ions are linked by BIDPE ligands and 5-OH- $bdc^{2-}$  anions to form infinitely double-stranded 1D chain (Fig. 21c). The  $Mn^{II}$  atoms were bridged by carboxylate ligands to form a binuclear cluster, each binuclear Mn was connected by four 5-OH- $bdc^{2-}$  anions to form a 1D ladder-shaped chain, the BIDPE ligands share the binuclear Mn clusters with 5-OH- $bdc^{2-}$  anions to further generate an infinite 2D network (Fig. 21d).

In another case, three mixed-ligand MOFs have been prepared by assembling  $Co^{II}$ ,  $Cd^{II}$ ,  $Zn^{II}$  nitrate with  $H_2L$  (4,4'-dicarboxydiphenylamine) and BIBP (4,4'-bis(imidazol-1-yl)diphenyl),<sup>51</sup> namely,  $[Co(L)(BIBP) \cdot H_2O]_n$  (**34**),  $[Cd(L)(BIBP)]_n$  (**35**),  $[Zn(L)(BIBP)]_n$  (**36**). In complex **34**, the  $Co^{II}$  ions are bridged by the BIBP ligands to afford 2D sheet, with the HL<sup>-</sup> decorating as arms (Fig. 22a). But for the **35** and **36**, the  $Cd^{II}$  and  $Zn^{II}$  ions can be regarded as 4-connected nodes with all crystallographically independent  $L^{2-}$  and BIBP ligands acting as linkers to form a (4,4) coordination sheet (Fig. 22b).

#### Conclusions

This paper outlined the influence factors on the assembly of MOFs. It can be seen that the positional isomerism, substituents and spacers of organic ligands have remarkable influence on the formation and structure of MOFs including the coordination mode with metal centers, the architecture topology, dimensionality and structural transformation and so on. It is also clear that the assembly, formation and structure of MOFs can differ greatly by some other factors including SBUs, solvents and metal ions. Nevertheless, we hope that this review can provide some primary information to the design and construction of desired MOFs.

#### Acknowledgements

We thank grants from the Natural Science Foundation of China (No. 21371092, 91022011) and the National Basic Research Program of China (2010CB923303).

State Key Laboratory of Coordination Chemistry, School of Chemistry and Chemical Engineering, Collaborative Innovation Center of Advanced Microstructures, Nanjing University, Nanjing 210093, P. R. China, E-mail: zhenghg@nju.edu.cn; Fax: +86 25 83314502

#### Notes and references

- L. G. Beauvais, J. R. Long, *J. Am. Chem. Soc.*, 2002, **124**, 12096.
- C. D. Wu, A. Hu, L. Zhang, W. Lin, *J. Am. Chem. Soc.*, 2005, **127**, 8940.
- M. Dincă, A. F. Yu, J. R. Long, *J. Am. Chem. Soc.*, 2006, **128**, 8904.
- R. Robson, *J. Chem. Soc., Dalton Trans.*, 2000, 3735.
- O. M. Yaghi, M. O'Keeffe, N. W. Ockwig, H. K. Chae, M. Eddaoudi, J. Kim, *Nature*, 2003, **423**, 705.
- Z. Zheng, H. Dong, J. F. Bai, Y. Z. Li, S. H. Li, M. Scheer, *J. Am. Chem. Soc.*, 2008, **130**, 7778.
- C. P. Li, M. Du, *Chem. Commun.*, 2011, **47**, 5958.
- D. F. Sun, S. Q. Ma, J. M. Simmons, J. R. Li, D. Q. Yuan, H. C. Zhou, *Chem. Commun.*, 2010, **46**, 1329.
- H. Sakamoto, R. Matsuda, S. Burekaew, D. Tanaka, S. Kitagawa, *Chem. - Eur. J.*, 2009, **15**, 4985.
- Y. Liang, M. Hong, W. Zhang, *Inorg. Chem.*, 2011, **40**, 4574.
- R. Bronisz, *Eur. J. Inorg. Chem.*, 2004, **18**, 3688.
- Q. Fang, G. Zhu, S. Qiu, *Dalton. Trans.*, 2004, **14**, 2202.
- I. S. Lee, D. M. Shin, Y. K. Chung, *Chem. - Eur. J.*, 2004, **10**, 3158.
- G. R. Desiraju, *Angew. Chem. Int. Ed.*, 2007, **46**, 8342.
- A. J. Blake, N. R. Champness, P. Hubberstey, W. S. Li, M. A. Withersby, M. Schroder, *Coord. Chem. Rev.*, 1999, **183**, 117.
- S. A. Barnett, N. R. Champness, *Coord. Chem. Rev.*, 2003, **246**, 145.
- (a) J. Fielden, D. L. Long, A. M. Z. Slawin, P. Kögerler, L. Cronin, *Inorg. Chem.*, 2007, **46**, 9090; (b) H. K. Liu, X.H. Huang, T. H. Lu, X. J. Wang, W. Y. Sun, B. S. Kang, *Dalton. Trans.*, 2008, 3178.
- Z. Zheng, H. Dong, J. F. Bai, Y. Z. Li, S. H. Li, M. Scheer, *J. Am. Chem. Soc.*, 2008, **130**, 7778.
- Y. Q. Tian, Y. M. Zhao, Z. X. Chen, G. N. Zhang, L. H. Weng, D. Y. Zhao, *Chem. - Eur. J.*, 2007, **13**, 4146.
- (a) Z. R. Pan, H. G. Zheng, T. W. Wang, Y. Song, Y. Z. Li, Z. J. Guo, S. R. Batten, *Inorg. Chem.*, 2008, **47**, 9528. (b) J. Wang, Z. J. Lin, Y. C. Ou, N. L. Yang, Y. H. Zhang, M. L. Tong, *Inorg. Chem.*, 2008, **47**, 190. (c) N. W. Ockwig, O. D. Friedrichs, M. O'Keeffe, O. M. Yaghi, *Acc. Chem. Res.*, 2005, **38**, 176. (d) H. Abourahma, B. Moulton, V. Kravtsov, M. J. Zaworotko, *J. Am. Chem. Soc.*, 2002, **124**, 9990.
- (a) J. S. Hu, L. F. Huang, X. Q. Yao, L. Qin, Y. Z. Li, Z. J. Guo, H. G. Zheng, Z. L. Xue, *Inorg. Chem.*, 2011, **50**, 2404. (b) Y. Qi, Y. X. Che, J. M. Zheng, *CrystEngComm*, 2008, **10**, 1137. (c) S. K. Henninger, H. A. Habib, C. Janiak, *J. Am. Chem. Soc.*, 2009, **131**, 2776.
- (a) H. A. Habib, J. Sanchiz, C. Janiak, *Inorg. Chim., Acta.*, 2009, **362**, 2452. (b) H. A. Habib, A. Hoffmann, H. A. Höpfe, C. Janiak, *Dalton. Trans.*, 2009, 1742. (c) H. A. Habib, J. Sanchiz, C. Janiak, *Dalton. Trans.*, 2008, 1734. (d) L. P. Zhang, J. Yang, J. F. Ma, Z. F. Jia, Y. P. Xie, G. H. Wei, *CrystEngComm.*, 2008, **10**, 1410. (e) S. C. Manna, K. I. Okamoto, E. Zangrando, N. R. Chaudhuri, *CrystEngComm.*, 2007, **9**, 199. (f) Z. F. Chen, S. F. Zhang, H. S. Luo, B. F. Abrahams, H. Liang, *CrystEngComm.*, 2007, **9**, 27.
- C. L. Zhang, M. D. Zhang, L. Qin, H. G. Zheng, *Cryst. Growth Des.*, 2014, **14**, 491.
- F. P. Huang, Z. M. Yang, P. F. Yao, Q. Yu, J. L. Tian, H. D. Bian, S. P. Yan, D. Z. Liao, P. Cheng, *CrystEngComm.*, 2013, **15**, 2657.
- Z. H. Zhang, S. C. Chen, J. L. Mi, M. Y. He, Q. Chen, M. Du, *Chem. Commun.*, 2010, **46**, 8427.

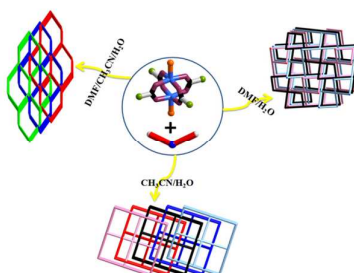
- 26 J. S. Hu, X. Q. Yao, M. D. Zhang, L. Qin, Y. Z. Li, Z. J. Guo, H. G. Zheng, Z. L. Xue, *Cryst. Growth Des.*, 2012, **12**, 3426.
- 27 M. Du, C. P. Li, C. S. Liu, S. M. Fang, *Coord. Chem. Rev.*, 2013, **257**, 1282.
- 5 28 M. Eddaoudi, J. Kim, N. Rosi, D. Vodak, J. Wachter, M. O'Keeffe, O. M. Yaghi, *Science.*, 2002, **295**, 469.
- 29 H. K. Chae, D. Y. S. Pérez, J. Kim, Y. Go, M. Eddaoudi, A. J. Matzger, M. O'Keeffe, O. M. Yaghi, *Nature.*, 2004, **427**, 523.
- 30 X. Q. Yao, M. D. Zhang, J. S. Hu, Y. Z. Li, Z. J. Guo, H. G. Zheng, *Cryst. Growth Des.*, 2011, **11**, 3039.
- 10 31 Z. Q. Shi, Y. Z. Li, Z. J. Guo and H. G. Zheng, *Cryst. Growth Des.*, 2013, **13**, 3078.
- 32 J. H. Cui, Y. Z. Li, Z. J. Guo and H. G. Zheng, *Cryst. Growth Des.*, 2012, **12**, 3610.
- 15 33 X. J. Li, F. L. Jiang, M. Y. Wu, L. Chen, J. J. Qian, K. Zhou, D. Q. Yuan, M. C. Hong, *Inorg. Chem.*, 2014, **53**, 1032.
- 34 J. L. C. Rowsell, E. C. Spencer, J. Eckert, J. A. K. Howard, O. M. Yaghi, *Science.*, 2005, **309**, 1350.
- 35 (a) S. S. Y. Chui, S. M. F. Lo, J. P. H. Charmant, A. G. Orpen, I. D. Williams, *Science.*, 1999, **283**, 1148. (b) B. Zheng, J. Bai, J. Duan, L. Wojtas, M. J. Zaworotko, *J. Am. Chem. Soc.*, 2011, **133**, 748.
- 20 36 J. H. Cui, Z. Z. Lu, Y. Z. Li, Z. J. Guo, H. G. Zheng, *Cryst. Growth Des.*, 2012, **12**, 1022.
- 37 J. H. Cui, Z. Z. Lu, Y. Z. Li, Z. J. Guo, H. G. Zheng, *Chem. Commun.*, 2012, **48**, 7967.
- 25 38 J. H. Cui, Y. Z. Li, Z. J. Guo, H. G. Zheng, *Chem. Commun.*, 2013, **49**, 555.
- 39 M. D. Zhang, H. G. Zheng, Z. Z. Lu, X. Q. Yao, *CrystEngComm.*, 2013, **15**, 9265.
- 30 40 Y. J. Huang, Y. L. Song, Y. Chen, H. X. Li, Y. Zhang, J. P. Lang, *Dalton Trans.*, 2009, 1411.
- 41 Z. Z. Lu, R. Zhang, Z. R. Pan, Y. Z. Li, Z. J. Guo, H. G. Zheng, *Chem. – Eur. J.*, 2012, **18**, 2812.
- 42 L. Qin, Z. Pan, L. Qian, Y. Li, Z. Guo and H. Zheng, *CrystEngComm.*, 2013, **15**, 5016.
- 35 43 K. Liang, H. Zheng, Y. Song, M. F. Lappert, Y. Li, X. Xin, Z. Huang, J. Chen, S. Lu, *Angew. Chem., Int. Ed.*, 2004, **43**, 5776.
- 44 Z. Pan, J. Xu, H. Zheng, K. Huang, Y. Li, Z. Guo, S. R. Batten, *Inorg. Chem.*, 2009, **48**, 5772.
- 40 45 Z. Z. Lu, R. Zhang, Y. Z. Li, Z. J. Guo, H. G. Zheng, *J. Am. Chem. Soc.*, 2011, **133**, 4172.
- 46 M. D. Zhang, L. Qin, X. Q. Yao, Q. X. Yang, Z. J. Guo, H. G. Zheng, *CrystEngComm*, 2013, **15**, 7354.
- 47 Z. R. Pan, X. Q. Yao, H. G. Zheng, Y. Z. Li, Z. J. Guo, S. R. Batten, *CrystEngComm*, 2009, **11**, 605.
- 45 48 (a) Z. Majeed, K. C. Mondal, G. E. Kostakis, Y. H. Lan, C. E. Anson, A. K. Powell, *Chem. Commun.*, 2010, **46**, 2551; (b) J. Zhang, T. Wu, C. Zhou, S. M. Chen, P. Y. Feng, X. H. Bu, *Angew. Chem., Int. Ed.*, 2009, **48**, 2542; (c) M. O'Keeffe, *Angew. Chem., Int. Ed.*, 2009, **48**, 8182.
- 50 49 X. Q. Yao, Z. R. Pan, J. S. Hu, Y. Z. Li, Z. J. Guo, H. G. Zheng, *Chem. Commun.*, 2011, **47**, 10049.
- 50 Z. Z. Lu, R. Zhang, Y. Z. Li, Z. J. Guo, H. G. Zheng, *Chem. Commun.*, 2011, **47**, 2919.
- 55 51 Q. X. Yang, X. Q. Chen, J. H. Cui, J. S. Hu, M. D. Zhang, L. Qin, G. F. Wang, Q. Y. Lu, H. G. Zheng, *Cryst. Growth Des.*, 2012, **12**, 4072.
- 52 Q. X. Yang, X. Q. Chen, Z. J. Chen, Y. Hao, Y. Z. Li, Q. Y. Lu, H. G. Zheng, *Chem. Commun.*, 2012, **48**, 10016.
- 60 53 J. S. Hu, L. F. Huang, X. Q. Yao, L. Qin, Y. Z. Li, Z. J. Guo, H. G. Zheng, Z. L. Xue, *Inorg. Chem.*, 2011, **50**, 2404.

## For Table of Contents Use Only

Manuscript ID CE-HIG-10-2014-002150

Title: Critical factors influencing the structures and properties of metal-organic frameworks

### Colour graphic:



**Text:** This article highlights the recent advances of different factors influencing on the structures of MOFs.